

Box-counting dimension without boxes: Computing D_0 from average expansion rates

Paul So,¹ Ernest Barreto,¹ and Brian R. Hunt²

¹*Department of Physics and Astronomy and the Krasnow Institute for Advanced Study, George Mason University, Fairfax, Virginia 22030*

²*Department of Mathematics and Institute for Physical Science and Technology, University of Maryland, College Park, Maryland 20742*

(Received 20 October 1998; revised manuscript received 16 February 1999)

We propose an efficient iterative scheme for calculating the box-counting (capacity) dimension of a chaotic attractor in terms of its average expansion rates. Similar to the Kaplan-Yorke conjecture for the information dimension, this scheme provides a connection between a geometric property of a strange set and its underlying dynamical properties. Our conjecture is demonstrated analytically with an exactly solvable two-dimensional hyperbolic map, and numerically with a more complicated higher-dimensional nonhyperbolic map. [S1063-651X(99)09206-5]

PACS number(s): 05.45.Df, 47.53.+n, 87.10.+e

I. INTRODUCTION

Fractal dimensions are important quantities in characterizing the geometric structure of strange sets. In particular, they provide measures of the arbitrarily fine scale structure of invariant sets generated by chaotic processes. From a practical point of view, they also provide an estimate of the minimum number of degrees of freedom needed to describe the dynamical evolution of these chaotic systems.

One of the simplest and most intuitive definitions of the fractal dimension of a strange set is the box-counting dimension (or capacity dimension) D_0 [1–5]. Given a fractal set in a d -dimensional Euclidean space, D_0 gives the scaling between the number of d -dimensional ϵ boxes needed to cover the set completely, and the boxes' size ϵ . For a fractal set generated by a chaotic process, one can also define its information dimension D_1 [6] by weighting the ϵ boxes by the frequency with which a typical chaotic trajectory visits each box.

Both these definitions are based on the geometric structure of the strange set, and, in the case of D_1 , its associated probability distribution. They both involve the construction of a covering set with a grid of ϵ boxes. Direct application of these geometric definitions to chaotic dynamical systems is difficult, since as ϵ decreases it becomes impossible to determine all the ϵ boxes visited by a given trajectory from a finite amount of data. This problem is especially severe for the box-counting dimension, because it can depend heavily on regions infrequently visited by a typical trajectory.

The Kaplan-Yorke conjecture connects the information dimension D_1 to the Lyapunov exponents of the chaotic set [7–9]: it relates a geometric quantity of a strange set to the dynamical properties of the underlying chaotic process. Most importantly, since numerical algorithms for calculating Lyapunov exponents are in general more efficient than dimension calculations based on the counting of ϵ -boxes in d -dimensional space, the Kaplan-Yorke conjecture provides a direct and simple method to estimate the information dimension of a chaotic set.

Various attempts [9–13] have been made to formulate a generalized Kaplan-Yorke-type relationship for the spectrum of generalized Renyi dimensions D_q [6], which includes the

box-counting dimension ($q=0$) and the information dimension ($q=1$). However, for $q \neq 1$, it does not appear that D_q can be expressed in terms of a finite number of invariants of the dynamical system such as Lyapunov exponents. In fact, the Lyapunov partition function formalism of Refs. [12,13] suggests that, for typical attractors, D_q must be determined from a *family* of weighted average volume expansion rates depending on a real parameter.

In this paper, we first propose and discuss the following conjecture for an upper bound for the box-counting dimension D_0 in terms of average k -dimensional expansion rates $E_k, k=1, \dots, d$ (to be defined below) of a d -dimensional chaotic system:

$$D_0 \leq m + \frac{\ln E_m}{\ln E_m - \ln E_{m+1}}, \quad (1)$$

where m is the smallest integer less than d such that the average $(m+1)$ -dimensional expansion rate E_{m+1} is contracting, i.e., $E_{m+1} < 1$ [14]. (This upper bound is generally lower than the rigorous upper bound reported in Ref. [15].) We also introduce an iterative scheme that generates a sequence of decreasing upper bound estimates for D_0 . Numerical experiments show that convergence to within machine precision of the true D_0 usually occurs within a few iterations. This proposed scheme provides a more efficient method for estimating the box-counting dimension of a chaotic attractor than the direct application of the definition of box-counting dimension, especially in experimental situations.

The paper is organized as follows. We begin with a definition of the box-counting dimension, and provide a heuristic argument for our conjecture. In Sec. III, we show analytically that Eq. (1) holds for the generalized baker's map (a simple hyperbolic system). In Sec. IV, we describe the relationship of our conjecture to the partition function formalism. In Sec. V, we describe our iterative refining scheme and demonstrate that it converges to the true value of D_0 . Finally, in Sec. VI, we numerically estimate the box-counting dimension of a nonhyperbolic system (the Hénon map) using our proposed iterative scheme, and show that our calculated results agree well with previous results reported elsewhere

[13,16]. We also illustrate the utility of our procedure by calculating D_0 as a function of a system parameter for a four-dimensional map.

II. CONJECTURE FORMULATION

Assume that we have a d -dimensional dynamical system given by a d -dimensional invertible map $\mathbf{F}(\mathbf{x})$, and that it possesses a chaotic attractor. The box-counting dimension D_0 of the attractor is defined in the following way. First we partition the entire d -dimensional state space by a grid of d -dimensional cubes with size ϵ . We then count the number of ϵ cubes, $N(\epsilon)$, that contain points belonging to the attractor. The set of all nonempty cubes constitutes a cover for the attractor. With successively smaller values of ϵ , the number of cubes $N(\epsilon)$ increases. The box-counting dimension D_0 of the attractor is defined as the scaling exponent between $N(\epsilon)$ and ϵ as $\epsilon \rightarrow 0$,

$$D_0 = \lim_{\epsilon \rightarrow 0} \frac{\ln(N(\epsilon))}{\ln(1/\epsilon)}. \quad (2)$$

The second ingredient needed in the formulation of our conjecture is the concept of average expansion rates. For simplicity, we assume that the chaotic attractor is hyperbolic, meaning that the number of asymptotically stable and unstable directions is invariant for the entire attractor and that there are no neutrally stable points embedded in the attractor. Consider a collection of M_0 initial conditions chosen randomly from the attractor according to its natural measure μ . For a given initial condition \mathbf{x}_0^j in the set ($1 \leq j \leq M_0$), we can define a spectrum of *finite time expansion factors* [4,11]

$$\lambda_1 \geq \lambda_2 \geq \dots \geq \lambda_d, \quad (3)$$

which is an ordered sequence of the square roots of the eigenvalues of the real non-negative Hermitian matrix $[\mathbf{DF}^n(\mathbf{x}_0^j)]^\dagger \mathbf{DF}^n(\mathbf{x}_0^j)$. Here $\mathbf{DF}^n(\mathbf{x}_0^j)$ is the Jacobian matrix of the n -times iterated map $\mathbf{F}^n(\mathbf{x}_0^j)$, and \dagger denotes the transpose of a matrix. Since we assume that we have a hyperbolic attractor, then for large n there exists an integer $1 \leq m \leq d$ such that for all \mathbf{x}_0^j , $\lambda_1 \geq \dots \geq \lambda_m > 1$ and $1 > \lambda_{m+1} \geq \dots \geq \lambda_d$.

With these finite time expansion factors, we can define the local finite time k -dimensional volume expansion rates $L_k(\mathbf{x}_0^j, n) = \prod_{i=1}^k \lambda_i(\mathbf{x}_0^j, n)$. As a simple example, after n repeated applications of the map \mathbf{F} , the image of a small line segment originally centered at \mathbf{x}_0^j with an initial length of ϵ will have a stretched length approximately given by $\epsilon L_1(\mathbf{x}_0^j, n) = \epsilon \lambda_1(\mathbf{x}_0^j, n)$. The finite time local volume expansion rates $L_k(\mathbf{x}_0^j, n)$ will in general fluctuate in time and across the attractor. It is useful to define the following per-iterate *average expansion rates* over the natural measure μ :

$$E_k = \lim_{n \rightarrow \infty} \langle L_k(\mathbf{x}_0^j, n) \rangle^{1/n} = \lim_{n \rightarrow \infty} \left(\lim_{M_0 \rightarrow \infty} \frac{1}{M_0} \sum_{j=1}^{M_0} L_k(\mathbf{x}_0^j, n) \right)^{1/n}. \quad (4)$$

It is important to note that although the asymptotic growth rate of $\lambda_i(\mathbf{x}_0^j, n)$ gives the Lyapunov exponents h_i of the

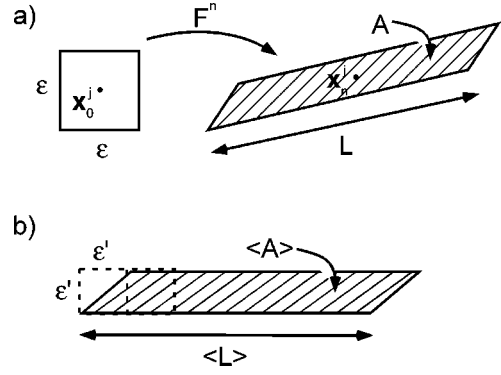


FIG. 1. (a) The j th ϵ box is stretched into a long thin parallelogram under the action of the map $\mathbf{F}^n(\mathbf{x}_0^j)$. The stretched box will have an area $A \sim \epsilon L_2(\mathbf{x}_0^j, n)$ and length $L \sim \epsilon L_1(\mathbf{x}_0^j, n)$. (b) Covering an average stretched ϵ box by boxes with smaller edge length $\epsilon' = \epsilon(E_2/E_1)^n$. $\langle A \rangle \sim \epsilon^2 E_2^n$ and $\langle L \rangle \sim \epsilon E_1^n$.

system [i.e., $h_i = \lim_{n \rightarrow \infty} (1/n) \ln \lambda_i(\mathbf{x}_0^j, n)$ for ‘‘almost every’’ \mathbf{x}_0^j with respect to the natural measure μ], E_k will typically be different from $\exp(\sum_{i=1}^k h_i)$ [17]. The difference will in general depend on the distribution of the finite time Lyapunov exponents [4]. While the Lyapunov exponents h_i are well recognized as important dynamical averages in studying chaotic systems, the average expansion rates E_k , to our knowledge, have received relatively little attention [12,13,18–20]. (An efficient method for calculating average expansion rates can be found in Ref. [19].)

To connect the geometric concept of the box-counting dimension D_0 of a chaotic attractor to its average expansion rates E_k , we consider a simple two-dimensional invertible map $\mathbf{F}(\mathbf{x})$ with $E_1 > 1$ and $E_2 < 1$. Thus, *on average*, a small line segment will be stretched and a small area will be contracted under the repeated application of the map \mathbf{F} . As in the definition for D_0 , we first cover the entire attractor with $\tilde{N}(\epsilon)$ boxes of edge length ϵ . We are interested in the additional number of boxes needed to cover the entire set if we decrease the size of the boxes. To estimate this scaling, we iterate each of the original ϵ boxes forward in time by a large number of iterates n . By choosing ϵ small enough, the images of the boxes are well approximated by a collection of stretched parallelograms; an example is shown in Fig. 1(a). The image of the box originally located at \mathbf{x}_0^j ($j \in [1, \tilde{N}(\epsilon)]$) will have a decreased area given by $\epsilon^2 L_2(\mathbf{x}_0^j, n)$ and a stretched edge length of $\epsilon L_1(\mathbf{x}_0^j, n)$. We can approximate the set of all such parallelograms with a new covering set consisting of $\tilde{N}(\epsilon)$ long thin parallelograms of area $\epsilon^2 E_2^n$ and edge length ϵE_1^n . We now want to cover these parallelograms with smaller boxes of edge length $\epsilon' = \epsilon(E_2^n/E_1^n)$. This requires an additional factor of $\epsilon E_1^n/\epsilon' = E_1^{2n}/E_2^n$ more ϵ' boxes to cover the entire attractor; see Fig. 1(b). Thus

$$\tilde{N}(\epsilon') \sim \frac{E_1^{2n}}{E_2^n} \tilde{N}(\epsilon). \quad (5)$$

Now we assume that $\tilde{N}(\epsilon)$ satisfies the following scaling relation with a dimensionlike exponent D_a : $\tilde{N}(\epsilon) \sim \epsilon^{-D_a}$ [21]. Then the above equation gives

$$\left(\frac{E_2^n}{E_1^n} \right)^{-D_a} \sim \frac{E_1^{2n}}{E_2^n} \epsilon^{-D_a}. \quad (6)$$

Solving for D_a , one obtains

$$D_a = 1 + \frac{\ln E_1}{\ln E_1 - \ln E_2}. \quad (7)$$

A similar derivation for D_a can be made for a d -dimensional invertible map with average m -dimensional expansion rate larger than 1 and an average $(m+1)$ -dimensional expansion rate less than 1. In this case, the n th iterated image of a d -dimensional ϵ cube will be approximately a stretched and squashed $(m+1)$ -dimensional parallelepiped. The average such parallelepiped will have an $(m+1)$ -dimensional volume $\sim \epsilon^{m+1} E_{m+1}^n$, while its largest m -dimensional face will have a volume $\sim \epsilon^m E_m^n$. Then, by considering the covering of this stretched and squashed parallelepiped with cubes of smaller edge length $\epsilon' = \epsilon(E_{m+1}^n/E_m^n)$, one obtains

$$D_a = m + \frac{\ln E_m}{\ln E_m - \ln E_{m+1}} \quad (8)$$

by following the same steps as in Eqs. (5)–(7). In this general case, the additional number of smaller ϵ' cubes needed will approximately scale as $\epsilon^m E_m^n / \epsilon'^m$.

The heuristic argument above suggests that D_a should approximate D_0 well in cases where the finite time Lyapunov exponents are nearly uniform across the attractor. Further analysis and numerical evidence, to be discussed below, suggests that, in general, Eq. (1) gives an upper bound on D_0 , i.e.,

$$D_a \geq D_0. \quad (9)$$

III. ANALYTICALLY TRACTABLE EXAMPLE

To demonstrate our conjecture in an analytically tractable hyperbolic system, we use the generalized baker's map [3,4] defined by the following transformation on the unit square $[0,1] \times [0,1]$:

$$x_{n+1} = \begin{cases} \lambda_a x_n & \text{if } y_n < \alpha \\ (1 - \lambda_b) + \lambda_b x_n & \text{if } y_n > \alpha, \end{cases} \quad (10a)$$

$$y_{n+1} = \begin{cases} y_n / \alpha & \text{if } y_n < \alpha \\ (y_n - \alpha) / \beta & \text{if } y_n > \alpha, \end{cases} \quad (10b)$$

where $\alpha + \beta = 1$ and $\lambda_a + \lambda_b \leq 1$. Starting with any initial point (x_0, y_0) within the unit square, after n iterates this map will have two finite time expansion factors

$$\lambda_1(m, n) = \alpha^{-m} \beta^{-(n-m)} > 1, \quad (11a)$$

$$\lambda_2(m, n) = \lambda_a^m \lambda_b^{n-m} < 1, \quad (11b)$$

where $m = 0, \dots, n$ is an integer that depends on the initial point (x_0, y_0) . In order to compute the average expansion rates with respect to the natural measure μ , we need to consider the repeated application of this map to a unit square.

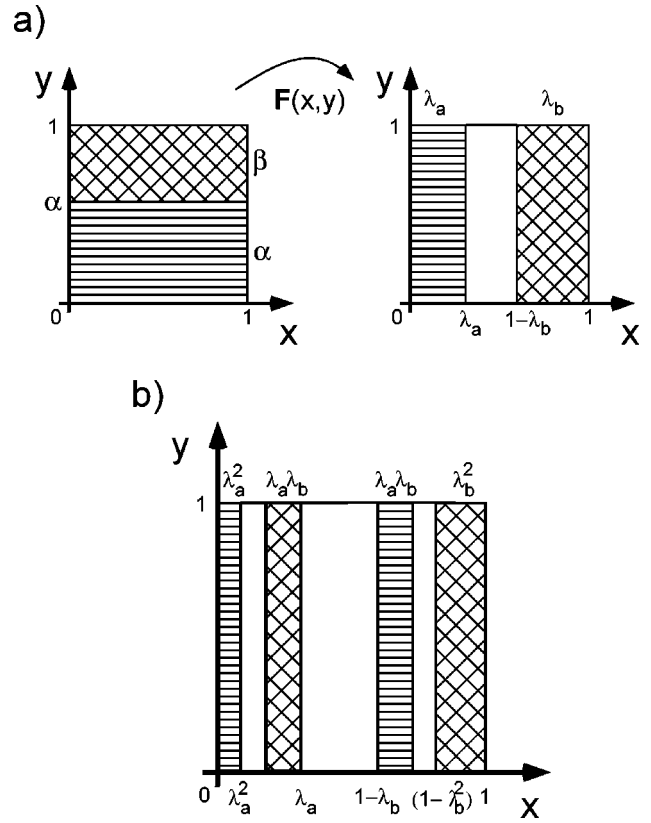


FIG. 2. Images of a unit square under the action of the generalized baker's map. (a) One iteration. (b) Two iterations.

After one iteration, a unit square will be mapped into two vertical strips with widths λ_a and λ_b , as shown in Fig. 2(a). By repeating the process once more, there will be four strips with widths λ_a^2 , $\lambda_a \lambda_b$, and λ_b^2 [see Fig. 2(b)]. After n iterations, the original unit square will become 2^n vertical strips with varying widths $\lambda_a^m \lambda_b^{n-m}$, $m = 0, \dots, n$. It can be shown that the number of strips $Z(m, n)$ with width $\lambda_a^m \lambda_b^{n-m}$ is given by the binomial coefficient $n! / (n-m)! m!$, and the natural measure for a given strip with width $\lambda_a^m \lambda_b^{n-m}$ (the fraction of area in the original unit square being mapped into the strip after n steps) is given by $\alpha^m \beta^{n-m}$. Thus the natural measure $\mu(m, n)$, containing all strips with width $\lambda_a^m \lambda_b^{n-m}$, is given by

$$\mu(m, n) = \alpha^m \beta^{n-m} \frac{n!}{(n-m)! m!}. \quad (12)$$

With the natural measure explicitly given by the above equation, we can compute the average expansion rates with Eq. (11). Specifically, the average finite time one-dimensional expansion rate $\langle L_1(m, n) \rangle$ is given by

$$\begin{aligned} \langle L_1(m, n) \rangle &= \langle \lambda_1(m, n) \rangle = \sum_{m=0}^n \mu(m, n) \alpha^{-m} \beta^{-(n-m)} \\ &= \sum_{m=0}^n \frac{n!}{(n-m)! m!} = 2^n. \end{aligned} \quad (13)$$

The last equality is true by virtue of the binomial theorem $2^n = (1+1)^n = \sum_{m=0}^n [n! / (n-m)! m!] 1^n 1^m$. This then gives

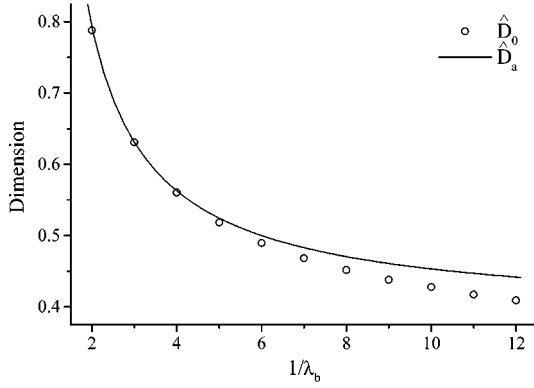


FIG. 3. Graph showing $\hat{D}_a \geq \hat{D}_0$ for the generalized baker's map. The solid line is the graph of \hat{D}_a using Eq. (15); open circles are numerically solved values of \hat{D}_0 using the transcendental equation (16) at selected values of λ_b . The other parameters are fixed at $\alpha = \frac{1}{3}$, $\beta = 1 - \alpha$, and $\lambda_a = \frac{1}{3}$. Note that $D_0 = D_a$ for $\lambda_b = \lambda_a = \frac{1}{3}$.

$E_1 = \lim_{n \rightarrow \infty} \langle L_1(n) \rangle^{1/n} = 2$. Similarly, we can calculate the average finite time area expansion rate

$$\begin{aligned} \langle L_2(m, n) \rangle &= \langle \lambda_1(m, n) \lambda_2(m, n) \rangle \\ &= \sum_{m=0}^n \mu(m, n) \frac{\lambda_a^m \lambda_b^{n-m}}{\alpha^m \beta^{n-m}} \\ &= \sum_{m=0}^n \frac{n!}{(n-m)! m!} \lambda_a^m \lambda_b^{n-m} \\ &= (\lambda_a + \lambda_b)^n. \end{aligned} \quad (14)$$

Again, the last equality is true by virtue of the binomial theorem, and $E_2 = \lim_{n \rightarrow \infty} \langle L_2(n) \rangle^{1/n} = \lambda_a + \lambda_b$. Then, by substituting E_1 and E_2 into Eq. (7), we have an explicit expression for D_a :

$$D_a = 1 + \frac{\ln 2}{\ln 2 - \ln(\lambda_a + \lambda_b)}. \quad (15)$$

Next we show that D_a is an upper bound for the box-counting dimension D_0 .

We now consider the box-counting dimension of the generalized baker's map by directly applying the box-counting definition [Eq. (2)]. Since the invariant set of the generalized baker's map is the product of a Cantor set (in the horizontal direction) and the unit interval $[0, 1]$ (in the vertical direction), the y direction will be smooth (of dimension 1), and the fractal contribution to D_0 will be solely from the x direction. Thus $D_0 = 1 + \hat{D}_0$, where \hat{D}_0 gives the scaling of the ϵ intervals needed to cover the Cantor set on the x axis. One way to calculate \hat{D}_0 is to utilize the scale invariant property of the map. \hat{D}_0 can be shown to be given by the transcendental equation [3,4]

$$\lambda_a^{\hat{D}_0} + \lambda_b^{\hat{D}_0} = 1. \quad (16)$$

Figure 3 is a graph of $\hat{D}_a = D_a - 1$ and the (numerical) solution to the above equation for \hat{D}_0 as a function of vary-

ing contraction rates λ_b (we fix λ_a at $\frac{1}{3}$ for this study). In the special case when $\lambda_a = \lambda_b$, Eq. (16) can be solved explicitly to give $\hat{D}_0 = -\ln 2 / \ln \lambda_a$, and the conjectured upper bound is a strict equality, i.e., $\hat{D}_0 = \hat{D}_a$. This is illustrated in Fig. 3 when $\lambda_a = \lambda_b = \frac{1}{3}$ and $\hat{D}_0 = \hat{D}_a = \ln 2 / \ln 3$. For asymmetric values of λ_a and λ_b , \hat{D}_0 and \hat{D}_a separate, and the curve \hat{D}_a given by Eq. (15) becomes an upper bound for \hat{D}_0 .

IV. PARTITION FUNCTION FORMALISM

One can analytically argue that in general, $D_a \geq D_0$ by utilizing the formalism used in Refs. [12,13]. In this formalism, D_0 is determined by considering the following "Lyapunov partition function" constructed from average (with respect to the natural measure) finite time expansion factors,

$$\gamma(\zeta, n) = \langle \lambda_1 \lambda_2^\zeta \rangle \quad (17)$$

where $0 \leq \zeta \leq 1$. For the generalized baker's map, $\gamma(\zeta, n)$ can be written explicitly in terms of λ_a and λ_b [see Eq. (11)],

$$\gamma(\zeta, n) = \sum_{m=0}^n \mu(m, n) \frac{\lambda_a^m \lambda_b^{\zeta(n-m)}}{\alpha^m \beta^{n-m}} = (\lambda_a^\zeta + \lambda_b^\zeta)^n, \quad (18)$$

where $\mu(m, n)$ is given by Eq. (12).

Defining

$$\Gamma(\zeta) \equiv \lim_{n \rightarrow \infty} (\gamma(\zeta, n))^{1/n} = \lambda_a^\zeta + \lambda_b^\zeta \quad (19)$$

and comparing the above equation with the transcendental equation, Eq. (16) for \hat{D}_0 , one observes that

$$\Gamma(\zeta) = \lambda_a^\zeta + \lambda_b^\zeta = 1 \quad \text{for } \zeta = \hat{D}_0. \quad (20)$$

More generally, for typical attractors of two-dimensional chaotic systems, the authors of Refs. [12,13] conjecture that if \hat{D}_0 is defined by

$$\gamma(\zeta) \begin{cases} \rightarrow \infty & \text{for } 0 \leq \zeta < \hat{D}_0 \\ \rightarrow 0 & \text{for } \hat{D}_0 < \zeta \leq 1; \end{cases} \quad (21)$$

then $D_0 = 1 + \hat{D}_0$. In terms of Γ , this is equivalent to

$$\Gamma(\zeta) \begin{cases} > 1 & \text{for } 0 \leq \zeta < \hat{D}_0 \\ = 1 & \text{for } \zeta = \hat{D}_0 \\ < 1 & \text{for } \hat{D}_0 < \zeta \leq 1. \end{cases} \quad (22)$$

We show below that $\hat{D}_a = D_a - 1 \geq \hat{D}_0$, and hence $D_a \geq D_0$ (provided the above conjecture holds), by showing that $\Gamma(\hat{D}_a) \leq 1$.

By the Hölder inequality [22], one can establish the following upper bound for the partition function within the range $\zeta \in [0, 1]$

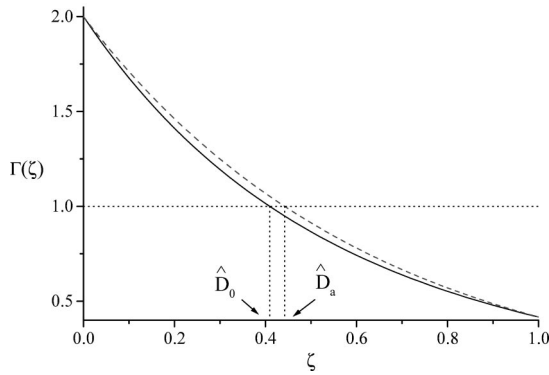


FIG. 4. The solid line is a graph of $\Gamma(\zeta)$ vs ζ for the generalized baker's map with $\alpha = \frac{1}{3}$, $\beta = 1 - \alpha$, $\lambda_a = \frac{1}{3}$, and $\lambda_b = \frac{1}{12}$; $\Gamma = 1$ at $\zeta = \hat{D}_0$. The dotted line is the upper bound $\Gamma_u(\zeta) = E_1(E_2/E_1)^\zeta$. This curve crosses $\Gamma = 1$ at our conjectured upper bound \hat{D}_a .

$$\begin{aligned} \gamma(\zeta, n) &= \langle \lambda_1 \lambda_2^\zeta \rangle = \langle \lambda_1^{1-\zeta} (\lambda_1 \lambda_2)^\zeta \rangle \\ &\leq \langle \lambda_1 \rangle^{1-\zeta} \langle \lambda_1 \lambda_2 \rangle^\zeta = \langle \lambda_1 \rangle \left(\frac{\langle \lambda_1 \lambda_2 \rangle}{\langle \lambda_1 \rangle} \right)^\zeta. \end{aligned} \quad (23)$$

Then, recalling that $L_1 = \lambda_1$ and $L_2 = \lambda_1 \lambda_2$ and taking the limit $n \rightarrow \infty$, we have the following upper bound for $\Gamma(\zeta)$:

$$\Gamma(\zeta) \equiv \lim_{n \rightarrow \infty} (\gamma(\zeta, n))^{1/n} \leq \lim_{n \rightarrow \infty} \langle L_1 \rangle^{1/n} \left(\frac{\langle L_2 \rangle}{\langle L_1 \rangle} \right)^{\zeta/n} = E_1 \left(\frac{E_2}{E_1} \right)^\zeta. \quad (24)$$

Because the above inequality is an upper bound for $\Gamma(\zeta)$ in the range $\zeta \in [0, 1]$, we can obtain an upper bound for \hat{D}_0 by solving

$$\Gamma_u(\zeta) \equiv E_1 \left(\frac{E_2}{E_1} \right)^\zeta = 1.$$

The solution to the above equation is precisely the fractional part \hat{D}_a of the dimensionlike quantity $D_a = 1 + \hat{D}_a$ in our conjecture [Eq. (7)]:

$$\hat{D}_a = \frac{\ln E_1}{\ln E_1 - \ln E_2}. \quad (25)$$

See Fig. 4 for a graph of $\Gamma(\zeta)$ and its upper bound $\Gamma_u(\zeta)$. By construction, \hat{D}_a will be an upper bound for \hat{D}_0 . In our example of the generalized baker's map with parameters $\alpha = \frac{1}{3}$, $\beta = 1 - \alpha$, $\lambda_a = \frac{1}{3}$, and $\lambda_b = \frac{1}{12}$, the value of D_0 calculated using the transcendental equation (16) is 0.409 and the estimated upper bound using our conjecture [Eq. (15)] is 0.442.

V. ITERATIVE SCHEME FOR REFINING ESTIMATE

One can successively obtain better estimates for \hat{D}_0 by an iterative procedure in the spirit of Newton's method. The procedure, which generates a sequence of estimates $\{\hat{D}_a^k\}$, $k = 1, 2, \dots$, is based on the observation that $\Gamma(\zeta)$ is a convex function [by which we mean that $\Gamma''(\zeta) > 0$]. Recall that \hat{D}_0 is given by the value of ζ where $\Gamma(\zeta) = 1$. Then, with the

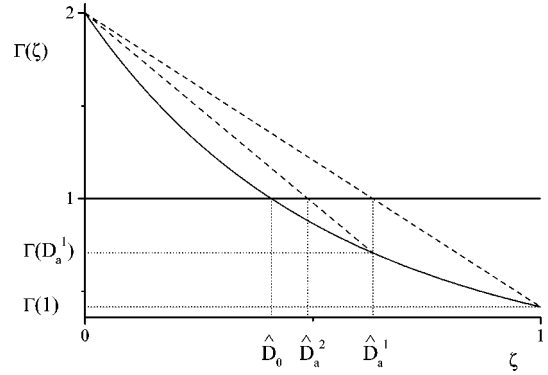


FIG. 5. By exploiting the concavity of $\Gamma(\zeta)$ (solid curve), straight lines may be used to estimate \hat{D}_0 . Here, \hat{D}_a^1 is the value of ζ where a straight line connecting $\Gamma(0)$ and $\Gamma(1)$ intersects $\Gamma(\zeta) = 1$. \hat{D}_a^2 is similarly obtained by using the straight line connecting $\Gamma(0)$ and $\Gamma(\hat{D}_a^1)$.

particular expansion rates [see Eq. (17)]

$$\Gamma(0) = \lim_{n \rightarrow \infty} \langle \lambda_1 \rangle^{1/n} = E_1,$$

$$\Gamma(1) = \lim_{n \rightarrow \infty} \langle \lambda_1 \lambda_2 \rangle^{1/n} = E_2,$$

a simple estimate \hat{D}_a^1 is obtained by the value of ζ where a straight line through $\Gamma(0)$ and $\Gamma(1)$ crosses 1. One may then obtain an improved estimate \hat{D}_a^2 by calculating $\Gamma(\hat{D}_a^1)$, and using the straight line through $\Gamma(0)$ and $\Gamma(\hat{D}_a^1)$. Figure 5 illustrates the procedure. Clearly, the sequence of estimates generated by this procedure converges to \hat{D}_0 .

An improved sequence of decreasing upper-bound estimates may be obtained by using more appropriate curves than the straight lines used above. A superior set of curves is suggested by Eq. (24) and its geometric interpretation in Fig. 4. There, we showed that our conjecture [Eq. (1)], is equivalent to estimating \hat{D}_0 by the value of ζ where

$$\Gamma_u(\zeta) = E_1 \left(\frac{E_2}{E_1} \right)^\zeta = \langle \lambda_1 \rangle \left(\frac{\langle \lambda_1 \lambda_2 \rangle}{\langle \lambda_1 \rangle} \right)^\zeta = 1.$$

Call the resulting estimate \hat{D}_a^1 . Using this value, we may apply the Hölder inequality to the partition function γ as follows:

$$\begin{aligned} \gamma(\zeta, n) &= \langle \lambda_1 \lambda_2^\zeta \rangle \\ &= \langle \lambda_1^{1-\zeta/\hat{D}_a^1} (\lambda_1 \lambda_2^{\hat{D}_a^1})^{\zeta/\hat{D}_a^1} \rangle \\ &\leq \langle \lambda_1 \rangle^{1-\zeta/\hat{D}_a^1} \langle \lambda_1 \lambda_2^{\hat{D}_a^1} \rangle^{\zeta/\hat{D}_a^1} \\ &= \langle \lambda_1 \rangle \left(\frac{\langle \lambda_1 \lambda_2^{\hat{D}_a^1} \rangle}{\langle \lambda_1 \rangle} \right)^{\zeta/\hat{D}_a^1}, \end{aligned} \quad (26)$$

which is valid for $\zeta \in [0, \hat{D}_a^1]$.

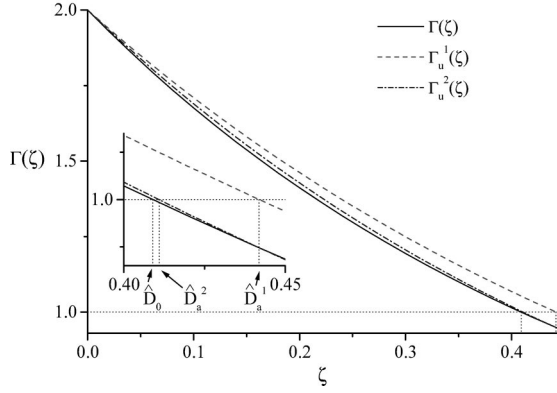


FIG. 6. Graph showing the construction of the second iterative upper-bound for $\Gamma(\zeta)$ using the two end points $\Gamma(0)$ and $\Gamma(\hat{D}_a^1)$, where $\hat{D}_a^1 = \ln E_1 / (\ln E_1 - \ln E_2)$ is our first iterative upper-bound estimate of \hat{D}_0 .

In addition, since $\langle \lambda_1 \lambda_2^{\hat{D}_a^1} \rangle \leq \langle \lambda_1 \rangle (\langle \lambda_1 \lambda_2 \rangle / \langle \lambda_1 \rangle)^{\hat{D}_a^1}$ by virtue of Eq. (23), we can also show the following inequality:

$$\begin{aligned} \langle \lambda_1 \rangle^{1-\zeta/\hat{D}_a^1} \langle \lambda_1 \lambda_2^{\hat{D}_a^1} \rangle^{\zeta/\hat{D}_a^1} &\leq \langle \lambda_1 \rangle^{1-\zeta/\hat{D}_a^1} \left[\langle \lambda_1 \rangle \left(\frac{\langle \lambda_1 \lambda_2 \rangle}{\langle \lambda_1 \rangle} \right)^{\hat{D}_a^1} \right]^{\zeta/\hat{D}_a^1} \\ &= \langle \lambda_1 \rangle \left(\frac{\langle \lambda_1 \lambda_2 \rangle}{\langle \lambda_1 \rangle} \right)^\zeta. \end{aligned} \quad (27)$$

Putting Eqs. (26) and (27) together, we have the desired sequence of inequalities:

$$\gamma(\zeta, n) \leq \langle \lambda_1 \rangle \left(\frac{\langle \lambda_1 \lambda_2^{\hat{D}_a^1} \rangle}{\langle \lambda_1 \rangle} \right)^{\zeta/\hat{D}_a^1} \leq \langle \lambda_1 \rangle \left(\frac{\langle \lambda_1 \lambda_2 \rangle}{\langle \lambda_1 \rangle} \right)^\zeta.$$

Taking the n th root of each term and letting $n \rightarrow \infty$, we obtain

$$\Gamma(\zeta) \leq \Gamma_u^2(\zeta) \leq \Gamma_u^1(\zeta),$$

where

$$\Gamma_u^1(\zeta) = \lim_{n \rightarrow \infty} \langle \lambda_1 \rangle^{1/n} \left(\frac{\langle \lambda_1 \lambda_2^{\hat{D}_a^1} \rangle}{\langle \lambda_1 \rangle} \right)^{\zeta/n} = E_1 \left(\frac{E_2}{E_1} \right)^\zeta,$$

$$\Gamma_u^2(\zeta) = \lim_{n \rightarrow \infty} \langle \lambda_1 \rangle^{1/n} \left(\frac{\langle \lambda_1 \lambda_2^{\hat{D}_a^1} \rangle}{\langle \lambda_1 \rangle} \right)^{\zeta/(\hat{D}_a^1 n)} = E_1 \left(\frac{\Gamma(\hat{D}_a^1)}{E_1} \right)^{\zeta/\hat{D}_a^1}.$$

These inequalities are represented by the concave curves in Fig. 6 (note the change of scale). Solving $\Gamma_u^1(\zeta) = 1$ gives our original estimate [Eq. (25)]

$$\hat{D}_a^1 = \frac{\ln E_1}{\ln E_1 - \ln E_2}.$$

Solving $\Gamma_u^2(\zeta) = 1$ gives an improved estimate

$$\hat{D}_a^2 = \hat{D}_a^1 \left(\frac{\ln E_1}{\ln E_1 - \ln \Gamma(\hat{D}_a^1)} \right).$$

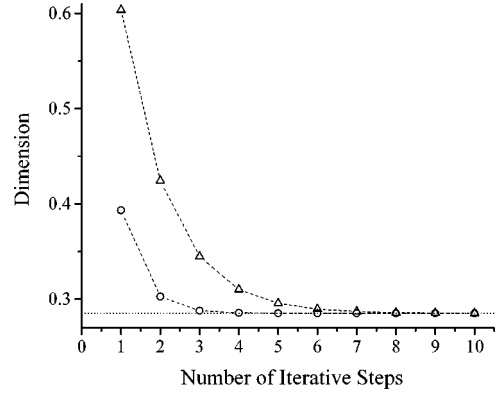


FIG. 7. Estimation of \hat{D}_0 with large asymmetric contraction rates ($\lambda_a = \frac{1}{3}$ and $\lambda_b = \frac{1}{100}$) using the iterative upper bound method. The dotted line is the numerically calculated \hat{D}_0 using Eq. (16), and the open circles are the iterative estimates \hat{D}_a^i of \hat{D}_0 using our procedure. The horizontal axis indicates the number of iterative steps.

Continuing the sequence in an analogous fashion, we solve

$$\Gamma_u^{i+1}(\zeta) \equiv E_1 \left(\frac{\Gamma(\hat{D}_a^i)}{E_1} \right)^{\zeta/\hat{D}_a^i} = 1$$

to obtain the $(i+1)$ th estimate

$$\hat{D}_a^{i+1} = \hat{D}_a^i \left(\frac{\ln E_1}{\ln E_1 - \ln \Gamma(\hat{D}_a^i)} \right).$$

This sequence of iterative upper bounds $\hat{D}_a^1 \geq \hat{D}_a^2 \geq \dots \geq \hat{D}_0$ must converge to \hat{D}_0 . Thus, operationally, instead of actually sampling the partition function $\Gamma(\zeta)$ as a function of ζ and looking for the location where it crosses 1, our iterative procedure provides a more efficient way to estimate the box-counting dimension by evaluating the partition function only at a few choice locations, namely, at $\zeta = 0, 1, \hat{D}_a^1, \hat{D}_a^2$, etc. Figure 7 is a demonstration of this iterative procedure in calculating the box-counting dimension of the generalized baker's map with $\lambda_a = \frac{1}{3}$ and $\lambda_b = \frac{1}{100}$ ($\alpha = \frac{1}{3}$ and $\beta = 1 - \alpha$). We choose these values since, recalling Fig. 3, we expect that the error between \hat{D}_0 and \hat{D}_a^1 should increase with increasing asymmetry between the two contraction rates λ_a and λ_b . This is indicated by the first open circle in Fig. 7. Although the percentage error of the first iterative upper bound estimate $\hat{D}_a^1 = 0.39334$ is relatively large ($\approx 38\%$), the sequence of iterative upper bounds \hat{D}_a^i converges very quickly to the actual value of $\hat{D}_0 = 0.28516$. Also plotted for comparison is the sequence of estimates obtained by using straight lines (triangles), as described at the beginning of this section.

VI. HIGHER-DIMENSIONAL NONHYPERBOLIC EXAMPLE

The generalized baker's map is a hyperbolic map with invariant hyperbolic subspaces. We now consider our itera-

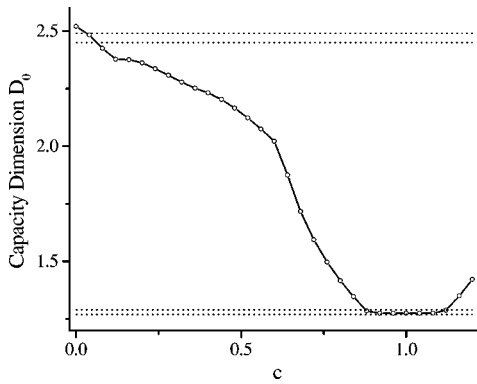


FIG. 8. Graph of D_0 for the coupled Hénon map as a function of the coupling parameter c . The lower dotted line is the box-counting dimension of a single Hénon attractor $D_0=1.28$. The upper dotted line is $2D_0=2.56$.

tive approximation method for a nonhyperbolic system, the Hénon map $\mathbf{H}(u, v; b) = (1.4 - u^2 + bv, u)$ with $b=0.3$. Using box-counting techniques, the box-counting dimension of the Hénon attractor was reported as 1.28 ± 0.01 [16]. Our estimate for D_0 using the iterative method is 1.2746 ± 0.0001 , in agreement. (At each iterative step in our estimation procedure, the average expansion rates were calculated using a single trajectory of 2×10^6 iterates, initiated at a randomly chosen initial condition within the basin of attraction. The final result is taken after the tenth refining step.) Using the partition formalism, Ott, Sauer, and Yorke obtain a D_0 estimate of 1.2745 ± 0.0005 [13], while Badii and Politi obtain a slightly higher value, 1.2755 ± 0.0005 [12]. While these results are consistent with each other at the extreme limits of the error bounds, our procedure supports the former result.

The relative simplicity of our procedure permits the easy calculation of an attractor's box-counting dimension as a function of a system parameter. To illustrate this, we use two nonidentical coupled Hénon maps

$$\mathbf{x}_{n+1} = \mathbf{H}(\mathbf{x}_n; b_x),$$

$$\mathbf{y}_{n+1} = (1-c)\mathbf{H}(\mathbf{y}_n; b_y) + c\mathbf{H}(\mathbf{x}_n; b_x),$$

where \mathbf{H} is the standard Hénon map (see above), c is the coupling parameter between the \mathbf{x} and \mathbf{y} subsystems, and we set $b_x=0.3$ and $b_y=0.2$. When $c=1$, the \mathbf{y} subsystem is completely enslaved by the \mathbf{x} subsystem, and D_0 for the combined system is just the box-counting dimension for a

single Hénon attractor with $b=0.3$. In Fig. 8, we plot the numerically estimated D_0 calculated using the iterative procedure of Sec. V as a function of coupling c . For each different value of the coupling and at each iterative step in our estimation procedure, the average expansion rates were calculated using a single trajectory of 2×10^6 iterates, initiated at a randomly chosen initial condition within the basin of attraction. The plotted estimates were obtained after ten refining steps.

In the case when $c=0$, the \mathbf{x} and \mathbf{y} dynamics decouple and the resulting attractor is the direct product of two non-identical Hénon attractors. Thus its dimension is the sum of the dimensions of each separate attractor, which we calculate to be 2.4740 ± 0.0001 by applying our algorithm to each Hénon map separately. In general, the case of two uncoupled systems is exceptional for the dimension formalism discussed here, due to the presence of Cantor-like structure along two independent directions. Accordingly, our algorithm for the full but decoupled system yields a slightly higher value, 2.5294 ± 0.0002 . For intermediate values of coupling, we expect the attractor to be Cantor-like in one direction only, and the formalism should be accurate. (A detailed description of the morphology of desynchronizing systems in terms of the changes in its topological entropy and dimensions will appear elsewhere [23].)

In summary, we propose Eq. (1) as an easy-to-calculate upper bound estimate for the box-counting dimension of a chaotic attractor. This is actually the first of a decreasing sequence of upper bounds for the box-counting dimension which we derive. The sequence is based on average expansion rates, quantities that are directly measurable from the observed dynamics of the chaotic process. This conjecture provides an interesting link between the geometric structure of a chaotic attractor to its underlying dynamical properties, and provides an efficient way to calculate the box-counting dimension of a chaotic set.

ACKNOWLEDGMENTS

We thank E. Ott and T. Sauer for helpful discussions. P.S. was supported by the National Institutes of Health under Grant No. 5-21215, and the National Science Foundation under Grant No. IBN-9727739. E.B. was supported in part by the National Science Foundation under Grant No. IBN-9727739. B.H. and E.B. were supported (in part) by the Department of Energy (Mathematical, Information, and Computational Sciences Division, High Performance Computing and Communications Program), and by the National Science Foundation (Divisions of Mathematical Sciences and Physics).

[1] A. N. Kolmogorov, Dok. Akad. Nauk. SSSR **119**, 861 (1958).
 [2] B. Mandelbrot, *Fractals: Form, Chance, and Dimension* (Freeman, San Francisco, 1977); *The Fractal Geometry of Nature* (Freeman, San Francisco, 1982).
 [3] J. D. Farmer, Physica D **7**, 153 (1983).
 [4] E. Ott, *Chaos in Dynamical Systems* (Cambridge University Press, New York, 1993).

[5] K. T. Alligood, T. D. Sauer, and J. A. Yorke, *Chaos: An Introduction to Dynamical Systems* (Springer-Verlag, New York, 1997), p. 174.
 [6] A. Renyi, *Probability Theory* (North-Holland, Amsterdam, 1970); P. Grassberger, Phys. Lett. A **97**, 227 (1983).
 [7] P. Frederickson, J. Kaplan, E. Yorke, and J. Yorke, J. Diff. Eqns. **49**, 185 (1983).

- [8] L.-S. Young, *Ergodic Theory Dyn. Syst.* **2**, 109 (1982).
- [9] P. Grassberger and I. Procaccia, *Physica D* **13**, 34 (1984).
- [10] P. Grassberger, in *Chaos*, edited by A. V. Holden (Manchester University Press, Manchester, 1986).
- [11] P. Grassberger, R. Badii, and A. Politi, *J. Stat. Phys.* **51**, 135 (1988).
- [12] R. Badii and A. Politi, *Phys. Rev. A* **35**, 1288 (1987).
- [13] E. Ott, T. Sauer, and J. A. Yorke, *Phys. Rev. A* **39**, 4212 (1989).
- [14] In the case when the average d -dimensional volume is expanding, i.e., $E_d > 1$, D_0 will be the dimension of the full state space, d .
- [15] B. R. Hunt, *Nonlinearity* **9**, 845 (1996).
- [16] P. Grassberger, *Phys. Lett. A* **97**, 224 (1983).
- [17] One can describe the fluctuations of the finite time Lyapunov number λ_i by a distribution function $P(\lambda_i)$, and in general $\ln \langle \lambda_i \rangle_P \neq \langle \ln \lambda_i \rangle_P$. Typically, $\ln E_1 \geq h_1$, $\ln aE_2 \geq h_1 + h_2$, and so on. A special case where $\ln E_1 = h_1$ is when the Jacobian matrix is constant over the attractor, as for the map $F(x) = 2x \pmod{1}$.
- [18] S. Newhouse, in *The Physics in Phase Space*, Lecture Notes in Physics Vol. 278 (Springer, Berlin, 1986); S. Newhouse and T. Pignataro, *J. Stat. Phys.* **72**, 1331 (1993).
- [19] J. Jacobs, E. Ott, and B. R. Hunt, *Phys. Rev. E* **57**, 6577 (1998).
- [20] The use of average expansion rates and topological entropy in examining the behavior of desynchronizing chaotic systems is described in Ref. [22].
- [21] We stress that since the new covering set is estimated rather than explicitly constructed, we do not expect that $D_a = D_0$. In fact, we demonstrate in Sec. IV that $D_a \geq D_0$.
- [22] The Hölder inequality states that $\langle fg \rangle \leq \langle f^s \rangle^{1/s} \langle g^t \rangle^{1/t}$, provided that $1/s + 1/t = 1$. In our case, we have $1/s = 1 - \zeta$, $1/t = \zeta$, $f = \lambda_1^{1-\zeta}$, and $g = (\lambda_1 \lambda_2)^\zeta$. E. Barreto, P. So, B. Gluckman, and S. Schiff (unpublished).
- [23] E. Barreto, P. So, B. Gluckman, and S. Schiff (unpublished).